Robust Controller Design of Hypersonic Vehicle in Uncertainty Models

Nan Wu and Jia Yu
1School of Aeronautic Science and Engineering, Beihang University, Beijing, China

Keywords: Hypersonic vehicle, robust controller, H_2/H_∞, norm,uncertainty models.

Abstract: This paper studies the controller of the air-breathing hypersonic vehicle. Taken the inertia into consideration, the control law of an air-breathing hypersonic vehicle is designed when the aircraft's appearance and aerodynamic parameters are changed. Due to the traditional controller is too dependent on the mathematic model of targets, the H_2/H_∞ control law of the air-breathing hypersonic vehicle is designed using the robust controller method. The rigid body model of the aircraft and the uncertainty model are researched in this paper. Then the corresponding robust controller is designed based on the uncertainty model in the case that the aircraft flies in different pitch angles. Finally, the stable flight characteristics of the hypersonic vehicle using the robust controller are verified in the complex flight conditions, compared to the general stability control system.

1 INTRODUCTION

Aspirated hypersonic vehicles have different degrees of uncertainty in their aerodynamics, propulsion and structure owing to their wide range of flight, complicated flight environment, fast flight speed and obvious aerodynamic heating effects (Bertin J J, 2003; Mcnamara J, 2011). Due to the integrated design, there is a strong coupling between subsystems such as aerodynamics, propulsion and structure (Cockrell C E, 2001). This coupling effect may amplify the uncertainty of the system, so that the aircraft dynamics characteristics deviate from the design goals, which even cause the control system failure. For example, X-43A is out of control in the first test flight because of uncertainty beyond the control system Stability boundary. The *LPV* method uses more modern control techniques in design and adopts norm-based performance measurement of control systems, control methods, singularity methods, and parametric methods based on decomposition. Among them, the influence of system uncertainty is fully considered, which has generality, is suitable for practical engineering application. However, this control method also has some negative defects, that is, it sacrifices other performance of the control system, resulting in poor dynamic mass of the system.

In the 1960s, a design method based on *LQG* feedback control was proposed. The optimal controller was designed, considering the dynamic performance, steady-state performance and control energy of the system. When the system was input with interference such as pulse and white noise, the output energy is the minimum, but the control method cannot guarantee the robustness of the system when there is uncertainty in the controlled system. Therefore, H_2/H_∞controller method is proposed, whose design idea is to combine H_∞ performance design with the H_2 performance design. As a result, the method make the closed-loop system has good robustness and excellent system performance (Zhang WeiGuo, 2012).

In this paper, a rigid body dynamics model of hypersonic vehicle is established for the problem of uncertainty of hypersonic vehicle. The H_2/H_∞ controller is designed to compare with the *K* feedback stabilization under the influence of uncertain parameters respectively, which can be used to verify the uncertainties problem.

2 HYPERSONIC AIRCRAFT RIGID BODY DYNAMICS MODEL

In this paper, the wave-rider configuration of the hypersonic vehicle is researched by establishing the rigid body model (Oppenheimer M, 2013; Bolender

Wu, N. and Yu, J.
Robust Controller Design of Hypersonic Vehicle in Uncertainty Models.
In *3rd International Conference on Electromechanical Control Technology and Transportation (ICECTT 2018)*, pages 288-293
ISBN: 978-989-758-312-4

M A, 2012; Parker J T, 2012). The layout of the aircraft is shown in Figure 1. Where L_f is the fore-body length; L_n is the engine length; L_a is the body length; δ_e is the elevator deflection; δ_c is canard deflection; τ_1 is the fore-body deflection; τ_2 is the body deflection.

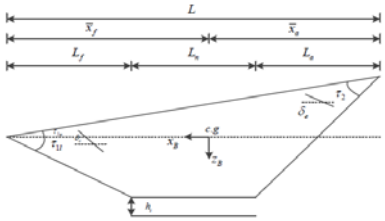

Figure 1 Hypersonic vehicle layout diagram

According to Lagrange equation, using a stable axis coordinate system, the hypersonic longitudinal rigid body dynamics model can be described as

$$\begin{cases} \dot{V} = \dfrac{X}{m} - g\sin(\theta-\alpha) \\ \dot{h} = V\sin(\theta-\alpha) \\ \dot{\alpha} = \dfrac{Z}{mV} + q + g\cos(\theta-\alpha)/V \\ \dot{q} = \dfrac{M}{I_y} \\ \dot{\theta} = q \end{cases} \quad (1)$$

Where V、h、α、q、θ are five rigid body state variables for hypersonic aircraft; m、M、I_y is the mass, moment and moment of inertia of the aircraft, respectively. Reference (AIAA, 2009) provides a curve fitting model of aerodynamic data, shown in Eq. (2).

$$\begin{cases} L \approx \bar{q}SC_L(\alpha,\delta_e,\delta_c) \\ D \approx \bar{q}SC_D(\alpha,\delta_e,\delta_c) \\ M \approx z_T T + \bar{q}S\bar{c}C_M(\alpha,\delta_e,\delta_c) \\ T \approx \bar{q}[\beta C_{T,\beta}(\alpha,M_{\infty}) + C_T(\alpha,M_{\infty})] \end{cases} \quad (2)$$

Where z_T is the thrust of the coupling coefficient of the moment; Three control input including elevator deflection angle δ_e, canard deflection δ_c and fuel equivalent ratio β; $C_{T,\beta}$ is the thrust coefficient and the ratio of fuel equivalence ratio; C_T is the thrust coefficient. Specific aerodynamic coefficients of the fitting expression can be detailed in reference 8.

The hypersonic aircraft flight Mach number is selected as 8Ma. The flight altitude is 85000ft. The given constraints are shown in table 1. The balance state is calculated using the hypersonic rigid body model as follows.

Table 1 the equilibrium state at the speed of 8Ma and the height of 85000ft

	Quantity of state	Array
Initial value	$[V\ \ h\ \ \alpha\ \ q\ \ \theta]$	[7846,85000,1,0,1]
Control input	$[\delta_e\ \ \beta]$	[3.9138, 0.5424]
Balance point	$[V\ \ h\ \ \alpha\ \ q\ \ \theta]$	[7846, 85000,1,0,1]
State derivate	$d[V\ \ h\ \ \alpha\ \ q\ \ \theta]$	1.0e-11*[0.60330,0,0,0,0]

Under this equilibrium state, characteristics root of air-breathing hypersonic aircraft is given in table 2. It can be seen from Table 2 that the rigid body model of the hypersonic vehicle is composed of a short-period mode, a long-period mode and a high-level mode. Among them, the short-period mode consists of two real poles distributed almost symmetrically with the imaginary axis, showing unstable characteristics. The long-period mode consists of a pair of complex conjugate poles, which are characterized by low frequency, under-damped. Its height-period modal is near the origin, which can be neglected. Thus, the aspirated hypersonic vehicle shows the characteristics of longitudinal instability. And the controller must be designed to control it to ensure the longitudinal stability of the hypersonic vehicle with good flight characteristics.

Table 2 The zero pole of hypersonic aircraft

Characteristic root	Damping ratio	Free frequency	Mode
$-2.6134\times10^{-5}\pm0.0365$	7.16×10^{-4}	0.0365	Long-period
-9.3822	1	9.3822	Short-period
9.2952	-1	9.2952	Short-period
-0.00205152	1	0.0020	Height-period

3 MODEL UNCERTAINTY ANALYSIS

In the process of modeling the air-breathing hypersonic vehicle， control law is designed easily for the longitudinal linear model, some ideal assumptions have to be made. Therefore, errors introduce uncertainty into the linear analysis model. These uncertainties have unpredictable interference with aircraft stability, maneuverability and control laws and may even cause serious accidents. Therefore, it is necessary to study in detail the uncertainties in the aircraft model. This paper summarizes the uncertain factors introduced in the

dynamics modeling process. The structural singular value method is selected to analyze the uncertainty parameters in the mode, considering the effects of these parameters on the vehicle.

As shown in Table 3, the corresponding mass, center of gravity, moment of inertia and change of structure elastic frequency of the aspirated hypersonic vehicle under different fuel conditions are given. On this basis, combined with the analysis of the modal characteristics, the range of uncertainty of each major uncertainty parameter is obtained.

Table 3 Uncertain parameters range in different fuel

Fuel	0%	30%	50%	70%	100%
$m(slug)$	93.57	126.1	147.9	169.6	202.2
$Iy\times10^5(slug.ft^2)$	1.56	2.102	2.465	2.827	3.37
$\bar{x}_f(ft)$	53.1	53.61	53.82	53.98	54.16
$\omega_1(rad/s)$	22.78	21.71	21.17	20.73	20.17
$\omega_2(rad/s)$	68.94	57.77	53.92	51.24	48.4
$\omega_3(rad/s)$	140	117.8	109.1	102.7	95.6

According to the analysis of references (Yujia, 2015), through the analysis and synthesis toolbox of Matlab, we can calculate the singular value of the system perturbed by the inertia factor, the aerodynamic parameters and the perturbation of the aircraft profile. The results show that the rigid hypersonic vehicle model is affected by inertia factors, aerodynamic parameters and aircraft shape.

4 H_2/H_∞ CONTROLLER DESIGN AND SIMULATION

Air breathing hypersonic vehicles have a wide range of flight, complex flight environment and fast flight speed. The dynamic model of the whole system has a wide range of changes, so that the structure and parameters of the flight control system will change as the vehicle changes. Considering the above characteristics, the flight control system of the aspirated hypersonic vehicle must meet the control requirements with large range of parameters and high uncertainty of the model.

Based on this requirement, the robust flight control design method is adopted to make the flight control system of the hypersonic vehicle have good robustness and excellent flight performance. H_2/H_∞ robust control method is used to control the aircraft, based on *LMI*.

4.1 H_2/H_∞ Control

The control idea of H_2/H_∞ is to combine the performance design of H_∞ and H_2 so that the closed-loop system has good robustness and good system performance. The H_2/H_∞ control structure is shown in Figure 2.

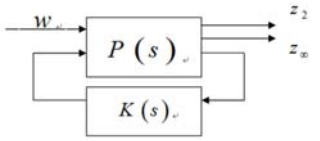

Figure 2 The definition of H_2/H_∞ control

Where *P (s)* is the generalized linear time plant structure, *K(s)* is the controller of H_2/H_∞. Equation 3 describes state equation of *P (s)*.

$$\begin{cases} \dot{x} = Ax + B_1 w + B_2 u \\ z_\infty = C_\infty x + D_{\infty 1} w + D_{\infty 2} u \\ z_2 = C_2 x + D_{21} w + D_{22} u \end{cases} \quad (3)$$

Where u is the control effectors variable; w is the uncertainty matrix input variable (including disturbance input, instruction input etc.); z_2 and z_∞ are output of H_2/H_∞. H_2 and H_∞ norm are defined as follows:

$$\|T(s)\|_2 = Trace\left(\frac{1}{2\pi}\int_{-\infty}^{\infty} T_{Z2w}(j\omega)T_{Z2w}^*(j\omega)d\omega\right)^{1/2} \quad (4)$$

Where T_{Z2w} is the transfer function from w to z_2; T_{Z2w}^* is the conjugate transposed matrix of T_{Z2w}; $Trace$ is the trace of the matrix. The square of H_2 norm is the system impulse response of the output energy.

$$\|T(s)\|_\infty = \sup_\omega \sigma_{\max}\left(T_{Z\infty w}(j\omega)\right) \quad (5)$$

Where $T_{Z\infty w}$ is the transfer function from w to z_∞. H_∞ norm represents the peak value of the maximum singular value of the system response frequency.

The state feedback controller can be expressed as

$$u = Kx \quad (6)$$

Substituting equation (6) into equation (3), the corresponding closed-loop system state space is described as:

$$\begin{cases} \dot{x} = (A + B_2 K)x + B_1 w \\ z_\infty = (C_\infty + D_{\infty 2} K)x + D_{\infty 1} w \\ z_2 = (C_2 + D_{22} K)x + D_{21} w \end{cases} \quad (7)$$

4.2 *LMI* Region and *D*-Stability

A basic problem in control theory and practice is to design a feedback control law that positions the poles of the closed-loop system in the desired position to ensure that the closed-loop system has the required dynamic and steady-state performance. However, due to the inaccuracy of the model and the existence of various disturbances, the poles of the closed-loop system should be placed in a suitable area on the complex plane.

The required regions are as follows: to ensure that the state response to the attenuation of the half-plane, the minimum damping ratio, the maximum natural frequency (Chilali M, 1996), shown in Figure 3. Adjusting this area can make the system's maximum overshoot, adjustment time, rise time, oscillation frequency and other time-domain response indicators meet the expected requirements. Eigenvalue area can use a Linear Matrix Inequality (LMI) to describe (Yuli, 2002).

In this paper, according to the relevant hypersonic vehicle data, the frequency is selected as 2～4 and the damping ratio is selected as 0.6～0.9. The final selected area is a sector centered at (-4,0), a radius of 4 and an included angle of 120 degrees.

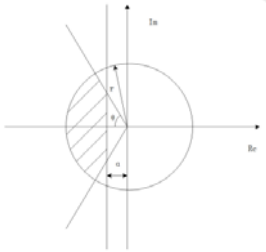

Figure 3 Closed-loop pole *LMI* area

4.3 Controller Design and Simulation

In this paper, the rigid body modes, rigid body dynamics and structural dynamics of the aspirated hypersonic vehicle are weakly coupled only between the short-period and the first-order elastic motions. That is, the rigid body modes do not excite the elastic modes and the aero-elasticity Modal will not stimulate rigid body mode. The H_2/H_∞ controller at the balance point is designed. The matrix parameters of generalized controlled system are as follows.

$$A = \begin{bmatrix} 0 & 0 & \text{-1.0953e2} & 0 & \text{-3.2150e1} \\ 0 & 0 & -7846 & 0 & 7846 \\ \text{-1.0572e-6} & \text{1.9419e-6} & \text{-1.2374e-1} & 1 & 0 \\ 0 & \text{-3.8714e-6} & \text{1.1101e1} & 0 & 0 \\ 0 & 0 & 0 & 1 & 0 \end{bmatrix}$$

$$B_1 = \begin{bmatrix} -0.0185 \\ -1 \\ -0.01589 \\ 0.0014 \\ -0.008 \end{bmatrix} \quad B_2 = \begin{bmatrix} -36.667 & 41.573 \\ 0 & 0 \\ -0.0161 & -0.0001 \\ -4.6860 & 0.0209 \\ 0 & 0 \end{bmatrix}$$

$$C_\infty = \begin{bmatrix} 0 & 0 & 0 & 0 & 0 \\ 0 & 0 & 0 & 0 & 0 \\ 0 & 0 & 1 & 0 & 0 \\ 0 & 0 & 0 & 1 & 0 \\ 0 & 0 & 0 & 0 & 0 \end{bmatrix} \quad C_2 = \begin{bmatrix} 0 & 1 & 0.7 & 1 & 0 \\ 0 & 0 & 0 & 0 & 0 \\ 1 & 1 & 0.5 & 0 & 0.2 \\ 1 & 1 & 0 & 0.5 & 0 \\ 0 & 0 & 0.1 & 0.1 & 0.8 \end{bmatrix}$$

$$D_{\infty 1} = D_{21} = \begin{bmatrix} 0 \\ 0 \\ 0 \\ 0 \\ 0 \end{bmatrix} \quad D_{\infty 2} = \begin{bmatrix} 0 & 0 \\ 0 & 0 \\ 0 & 0 \\ 0 & 0 \\ 0 & 0 \end{bmatrix} \quad D_{22} = \begin{bmatrix} 0 & 0 \\ 0 & 0 \\ 1 & 1 \\ 1 & 1 \\ 1 & 1 \end{bmatrix}$$

For hypersonic aircraft, the control system needs to give priority to ensuring robustness. For the H_∞ norm constrained optimization iteration of the generalized linear time-invariant system *P(s)*, we get the optimal threshold value of H_∞ norm is 0.24, which indicates that H_∞ norm is $\gamma_1 \geq 0.24$ in the final H_2/H_∞ design. By H_2 norm constrained optimization iteration of *P(s)*, the optimal H_2 norm value is 2.01, corresponding to H_∞ = 0.45. So H_∞ norm is selected as $0.24 \leq \gamma_1 \leq 0.45$.

When the H_∞ index γ_1 becomes larger, it can be seen that the system robustness becomes stronger and the dynamic performance is worse. So the choice of γ_1 needs to be taken into account. The H_2 and H_∞ nostrils are approximately inversely proportional. When the H_∞ norm increases to 0.4, the H_2 norm is almost invariant. So γ_1= 0.4 is selected, and the H_2 norm corresponding to this is taken as 2.55. The controller state matrix is:

$$A_K = \begin{bmatrix} -8.5487 & -1.1192 & 0.2161 & 0.1994 & -0.5475 \\ -28.5022 & -23.8086 & 4.0025 & 2.4283 & -1.5220 \\ -22.2929 & -11.9760 & -7.8630 & 5.2365 & -40.0805 \\ -84.6104 & -79.7104 & 22.6790 & 0.4907 & 36.8523 \\ -7.6919 & -7.0448 & 1.7637 & 0.8601 & -5.8979 \end{bmatrix}$$

$$B_K = \begin{bmatrix} -177.5367 & 4.5970 & -1.4933\times10^{3} & 28.5387 & 6.1444\times10^{3} \\ -2.9410\times10^{3} & -5.8339 & 6.8808\times10^{4} & -1.4759\times10^{3} & 1.0087\times10^{4} \\ -857.3554 & -11.3396 & 6.1016\times10^{4} & 1.5855\times10^{4} & -1.0071\times10^{4} \\ -1.3881\times10^{4} & -39.2010 & 4.9033\times10^{5} & -5.3110\times10^{4} & -3.0183\times10^{5} \\ -1.1164\times10^{3} & 4.6595 & -4.5228\times10^{4} & -1.9587\times10^{3} & 7.1836\times10^{4} \end{bmatrix}$$

$$C_K = \begin{bmatrix} 0.0013 & 6.2453\times10^{-4} & 2.0713\times10^{-4} & -4.0358\times10^{-4} & 0.0035 \\ 0.0027 & 0.0015 & -1.8815\times10^{-5} & -5.2469\times10^{-4} & 0.0035 \end{bmatrix}$$

$$D_K = \begin{bmatrix} 0 & 0 & 0 & 0 & 0 \\ 0 & 0 & 0 & 0 & 0 \end{bmatrix}$$

After the introduction of robust state feedback controller, the pole is -2.3545 ± 2.3076i. The short-period damping of the system is 0.714 and the frequency is 3.297. The variation of frequency shows that the dynamic characteristics of the system are improved. The damping increase indicates the robustness of the system increases. It can quickly return to equilibrium under external disturbance or system state changes.

In the following, an ordinary steady-state feedback K is introduced, compared with the state feedback of H_2/H_∞. It is verified that the H_2/H_∞ hybrid controller still guarantees a good control effect under the condition of large system uncertainty.

$$K = \begin{bmatrix} -0.0002 & 0.0799 & -110.3370 & -0.3480 & 113.5158 \\ -0.0007 & -0.0097 & -209.3452 & 0.4513 & 215.5714 \\ 0.1344 & 0.0741 & 25.2763 & -0.5639 & -30.5862 \end{bmatrix}$$

The system adds (1°, 1s) the elevator step response. Δ0 is the case of no parameter perturbation. Δ1, Δ2 are the two parameters perturbation of the cutoff, respectively. In figure 4, dotted line represents normal feedback K and solid line represents H_2/H_∞ mixed controller feedback. And The inertial parameters perturbation response is also shown.

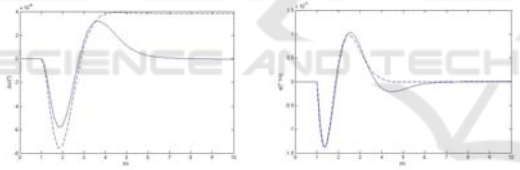

(1) Δ0 The angle of attack (2) Δ0 The rate of pitch

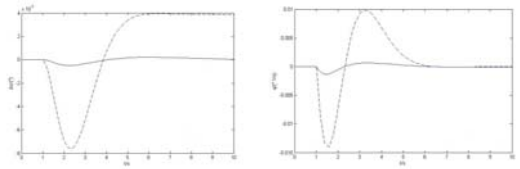

(3) Δ1 The angle of attack (4) Δ1 The rate of pitch

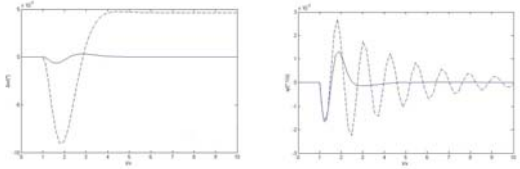

(5) Δ2 The angle of attack (6) Δ2 The rate of pitch

Figure 4

Taken the aerodynamic parameters into account, the system responds to (1°, 1s) the elevator's step response is shown in Fig.5.

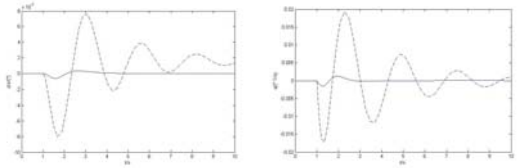

(1) Δ1 The angle of attack (2) Δ1 The rate of pitch

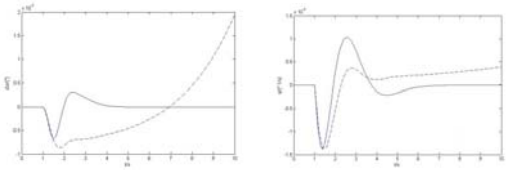

(3) Δ2 The angle of attack (4) Δ2 The rate of pitch

Figure 5

Taken the aircraft shape parameter into account, the system responds to (1°, 1s) the elevator's step response is shown in Fig.6.

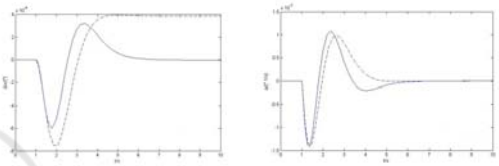

(1) Δ1 The angle of attack (2) Δ1 The rate of pitch

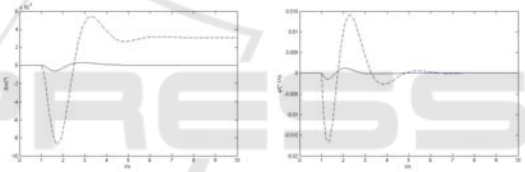

(3) Δ2 The angle of attack (4) Δ2 The rate of pitch

Figure 6

As can be seen from the response curves of each state in the figure, in the model with robust control, the angle of attack and the rate of pitch of the closed-loop system converge faster and have almost no oscillation after being perturbed. And the equilibrium state can be recovered faster. In the system with parameter perturbation, the closed-loop system can still maintain the stability. However, the amplitude of the shock is very large and even diverges after the parameter is perturbed without adding the model of robust control. It shows that the robust control closed-loop system is robust and has good maneuverability.

5 CONCLUSIONS

This article is aimed at uncertain control problems of aspirated hypersonic vehicle in flight, considering complicated flight environment and uncertainty of aerodynamic configuration. According to the results of the uncertainty analysis of the structure singular value method, a robust control method is used to

design the control law of a hypersonic vehicle considering the inertia, the aerodynamic parameters and the aircraft shape uncertainty. The simulation results are compared with the ordinary augmentation system. After adding the perturbation parameter, the response curves of the angle of attack and the rate of the pitch ordinary augmentation system fluctuate greatly and even the divergence occurs. The response curves of the pitch velocity of the robust control system converge very quickly, almost no shock. The comparison results show that the control law design of ordinary stabilization system cannot solve the problem of stability control of hypersonic vehicles with uncertainties. However, the H_2/H_∞ robust control method can solve this problem well and has good control effect.

REFERENCES

Bertin J J, Cummings R M. *Fifty years of hypersonics: where we've been, where we're going［J］. Progress in Aerospace Sciences*，2003, 39(6):511-536.

Mcnamara J, Friedmann P. *Aeroelastic and Aerothermoelastic Analysis in Hypersonic Flow: Past, Present, and Future［J］. Aiaa Journal*，2011，49(6):1089-1122.

Cockrell C E, Engelund W C, Bittner R D. *Integrated Aeropropulsive Computational Fluid Dynamics Methodology for the Hyper-X Flight Experiment［J］. Journal of Spacecraft & Rockets*， 2001, 38(6):836-843.

ZhangWeiGuo.*Robust flight control system design[M].Changsha.National defense industry press*,2012:page 105-136.

Oppenheimer M, Skujins T, Bolender M, et al. *A Flexible Hypersonic Vehicle Model Developed with Piston Theory[C]// AIAA Atmospheric Flight Mechanics Conference and Exhibit.* 2013.

Bolender M A, Doman D B. *Nonlinear Longitudinal Dynamical Model of an Air-Breathing Hypersonic Vehicle［J］. Journal of Spacecraft & Rockets*，2012，44(2):374-387.

Parker J T, Serrani A, Yurkovich S, et al. *Control-Oriented Modeling of an Air-Breathing Hypersonic Vehicle［J］. Journal of Guidance Control & Dynamics*，2012, 30(3):856-869.

AIAA. *Development Of Linear Parameter-Varying Models Of Hypersonic Air-Breathing Vehicles[C] AIAA Guidance, Navigation, and Control Conference*. 2009.

Yujia,Yangpengfei. *Hypersonic vehicle model uncertainty impact analysis[J].Journal of aviation.*2015,(1):192-200.

Chilali M,Gahinet P. *H∞ Design with Pole Placement Constraints: an LMI approach［J］.IEEE Transactions on Automatic Control*， 1996， 41(3):358-367.

Yuli.*Robust control,linear matrix inequality LMI approach[M].Beijing:Qinghua university press*,2002.

Zhang qing-jiang.*With regional pole assignment of H2/H∞ control [D].Xian:Nothwestern poly technical university,*2006.